ARR No. 3F23

NATIONAL ADVISORY COMMITTEE FOR AERONAUTICS

WARTIME REPORT

ORIGINALLY ISSUED

June 1943 as
Advance Restricted Report 3F23

WIND-TUNNEL INVESTIGATION OF EFFECT OF YAW ON LATERAL-STABILITY CHARACTERISTICS V - SYMMETRICALLY TAPERED WING WITH A CIRCULAR FUSELAGE HAVING A HORIZONTAL AND A VERTICAL TAIL

By Arthur R. Wallace and Thomas R. Turner

Langley Memorial Aeronautical Laboratory
Langley Field, Va.

NACA

WASHINGTON

NATIONAL ADVISORY COMMITTEE FOR AERONAUTICS

ADVANCE RESTRICTED REPORT

WIND-TUNNEL INVESTIGATION OF EFFECT OF YAW ON LATERAL-STABILITY CHARACTERISTICS V - SYMMETRICALLY TAPERED WING WITH A CIRCULAR FUSELAGE HAVING A HORIZONTAL AND A VERTICAL TAIL

By Arthur R. Wallace and Thomas R. Turner

SUMMARY

Tests were made in the LMAL 7- by 10-foot tunnel to determine the effect of a horizontal tail on the lateral-stability characteristics of a high-wing, a midwing, and a low-wing monoplane. The model combinations consisted of a circular fuselage, an NACA 23012 tapered wing, and an NACA 0009 horizontal tail surface. Each wing-fuselage combination was tested with a partial-span split flap neutral and deflected 60° and with and without a single vertical tail. Tests were also made of the fuselage with and without the tail surfaces.

The effect of the horizontal tail is shown in the presentation of the results in the form of increments of the rate of change in the coefficients of rolling moment, yawing moment, and lateral force with yaw caused by wing-fuselage interference. The coefficients at high angles of yaw for all model configurations are presented. The data are compared with data from similar model combinations without the horizontal tail.

The addition of the horizontal tail was found to reduce the variation of the wing-fuselage interference and the change in the effect of wing-fuselage interference on the vertical tail with vertical position of the wing on the fuselage. The presence of the horizontal tail increased the effective aspect ratio of the vertical tail by 20 to 60 percent, depending on the angle of attack. For angles of yaw larger than about 15° the horizontal tail slightly reduced the effectiveness of the vertical tail.

INTRODUCTION

Considerable data are available for the evaluation of the effect of aerodynamic interference between wing, fuselage, and vertical tail on lateral-stability characteristics (references 1, 2, and 3). These data indicate that the vertical-tail effectiveness is greater with the wing in a low position on the fuselage than with the wing in a high position. Air-flow surveys in the region of the vertical tail showed that the change in tail effectiveness with wing position resulted from a side flow the magnitude and direction of which were functions of wing position (reference 4). Because the data of references 1 to 4 were obtained for models without a horizontal tail, the question arises as to whether a horizontal tail will modify these results. The horizontal tail has been known to increase the effectiveness of the vertical tail by acting as an end plate. A theoretical analysis of this end-plate effect was made in reference 5.

The present report continues the investigation of lateral-stability characteristics by adding a fourth part, the horizontal tail, to the previous model consisting of a wing, fuselage, and vertical tail. The purpose of the present report is to determine to what extent the horizontal tail influences the effect of wing-fuselage interference on the vertical tail and to determine experimentally the end-plate effect of the horizontal tail on the vertical tail.

MODEL AND APPARATUS

The tests were made in the LMAL 7- by 10-foot tunnel with the regular six-component balance. The tunnel and the balance are described in references 6 and 7.

The model (fig. 1) was identical with the circular fuselage and symmetrically tapered wing model of reference 1 except for the addition of the horizontal tail surface. For the midwing combination the chord line of the wing was placed on the center line of the fuselage. For the high- and the low-wing combinations the surface of the wing was made tangent to the surface of the fuselage. The wing was set at 0° incidence with respect to the fuselage center line for all cases.

The 3:1 symmetrically tapered wing used in the tests was previously used in the investigation reported in reference 1. It has an NACA 23012 section and the maximum upper-surface ordinates are in one plane, with the result that the chord plane has a dihedral of 1.45°. The wing tips are formed of quadrants of approximately similar ellipses. The sweepback of the locus of quarter-chord points is 4.75°, the area is 4.1 square feet, and the aspect ratio is 6.1.

The fuselage is circular in cross section and was made to ordinates given in reference 1. Both tail surfaces are of NACA 0009 section and have areas which arbitrarily include a portion through the fuselage, as shown in figure 1. The horizontal-tail area is 97.8 square inches and the span is 20 inches, which gives a geometric aspect ratio of 4.1. The incidence of the horizontal tail was 0° with respect to the fuselage center line for all cases. The vertical-tail area is 53.7 square inches and the span measured to the center line of the fuselage is 10.87 inches, which gives a geometric aspect ratio of 2.2.

The split flaps, of 20 percent chord and 60 percent span, were made of 1/16-inch steel. For the high-wing and the midwing combinations, the flaps were cut to allow for the fuselage and the gaps between the fuselage and the flaps were sealed. The flaps were attached at a 60° deflection.

TESTS

The test procedure was similar to that described in references 1, 2, and 3. Tests were made of the fuselage alone, of the fuselage with horizontal tail, of the fuselage with vertical tail, and of the fuselage with both tail surfaces. Similar tail variations were tested with wing-fuselage combinations representing high-wing, midwing, and low-wing monoplanes. All wing-fuselage combinations were tested with and without flaps. The combinations were tested at angles of attack from −10° to 20° with the model yawed −5°, 0°, and 5°. A yaw range of −15° to 50° was investigated for most wing-fuselage combinations at an angle of attack 2° less than the angle of attack for maximum lift at 0° yaw.

A dynamic pressure of 16.37 pounds per square foot, which corresponds to a velocity of about 80 miles per hour, was maintained in all tests. The Reynolds number based on a mean wing chord of 9.84 inches was about 609,000. Based on a turbulence factor of 1.6 for the LMAL 7- by 10-foot tunnel, the effective Reynolds number was about 975,000.

RESULTS

The data are given in standard nondimensional coefficient form with respect to the center-of-gravity location shown in figure 1. The results are referred to a system of axes in which the X axis is the intersection of the plane of symmetry of the model with a plane perpendicular to the plane of symmetry and parallel to the relative wind direction, the Y axis is perpendicular to the plane of symmetry, and the Z axis is in the plane of symmetry and perpendicular to the X axis.

The coefficients for the fuselage alone and for the fuselage with tail surfaces are based on the wing dimensions. The coefficients are defined as follows:

C_L lift coefficient (lift/qS)

C_D drag coefficient (D/qS)

C_m pitching-moment coefficient $(M/q\bar{c}S)$

C_Y lateral-force coefficient (Y/qS)

C_{Y_ψ} slope of curve of lateral-force coefficient against yaw $(\partial C_Y/\partial\psi)$

C_l rolling-moment coefficient (L/qbS)

C_{l_ψ} slope of curve of rolling-moment coefficient against yaw $(\partial C_l/\partial\psi)$

C_n yawing-moment coefficient (N/qbS)

C_{n_ψ} slope of curve of yawing-moment coefficient against yaw $(\partial C_n/\partial\psi)$

Δ_1 ... change in partial derivatives caused by wing–fuselage interference. (Designates increments of C_{l_ψ}, C_{n_ψ}, or C_{Y_ψ})

Δ_2 change in vertical–tail effectiveness caused by wing–fuselage interference (Designates increments of C_{l_ψ}, C_{n_ψ}, or C_{Y_ψ})

where

L rolling moment

D drag

Y lateral force

M pitching moment

N yawing moment

q dynamic pressure ($1/2\ \rho V^2$)

V tunnel–air velocity

ρ air density

S wing area

S_f vertical–tail area

b wing span

$\bar{c}$ average wing chord

and

A_e effective aspect ratio of vertical tail

α angle of attack corrected to free stream, degrees

α' uncorrected angle of attack, degrees

ψ angle of yaw, degrees

δ_f angle of flap deflection, degrees

The subscript f refers to the vertical tail, except when used with δ.

Lift, drag, and pitching-moment coefficients for the various wing-fuselage arrangements are presented in figure 2. The values of α, C_D, and C_m shown in this figure were corrected to free air, but in all subsequent figures no corrections were made.

The corrections were computed as follows:

$$\Delta\alpha = 57.3\ \delta_w \frac{S}{C} C_L \quad \text{(deg.)}$$

$$\Delta C_D = \delta_w \frac{S}{C} C_L^2$$

$$\Delta C_m = 57.3 \left(\frac{1}{\sqrt{q/q_o}} \delta_T - \delta_w \right) \frac{S}{C} \frac{\partial C_m}{\partial i_t} C_L$$

where

δ_w jet-boundary correction for wing (0.117)

δ_T total jet-boundary correction at tail (0.179)

S wing area (4.1 sq ft)

C tunnel cross-sectional area (69.59 sq ft)

$\frac{q}{q_o}$ ratio of dynamic pressure at tail to free-stream dynamic pressure; assumed to be unity

$\frac{\partial C_m}{\partial i_t}$ change in pitching-moment coefficient per degree change in stabilizer setting as determined in tests

All corrections were additive.

The lateral-stability derivatives for component parts of the model appear in figure 3, which shows the end-plate effect of the horizontal tail on the vertical tail.

Another method illustrating the effect of the horizontal tail on the vertical tail is to treat the increased effectiveness of the vertical tail as an increase in effective aspect ratio, as was done in reference 5. This method can be used by employing a relation between aspect ratio and slope of the lift curve. A formula for giving this relation that gives one of the best agreements with experimental values is given in reference 8.

$$a = a_o \frac{A}{EA + 2}$$

When solved for the aspect ratio A, this equation gives an effective aspect ratio which will be termed A_e

$$A_e = \frac{2a}{a_o - Ea} \qquad (1)$$

where

a_o slope of lift curve for infinite aspect ratio (0.1 per degree is a representative experimental value for an NACA 0009 airfoil)

a slope of lift curve for vertical tail ($a = \frac{S}{S_f} C_{Y_{\psi_f}}$ per degree, where the arbitrary selection of S_f is shown in fig. 1)

E ratio of semiperimeter to span of an elliptic plate of aspect ratio A

The value of $C_{Y_{\psi_f}}$ was obtained directly from the force measurements and also indirectly from the yawing-moment measurements by use of the equation

$$C_{Y_{\psi_f}} = -C_{n_{\psi_f}} \frac{b}{l_f} \qquad (2)$$

where

$C_{Y_{\psi_f}}$ = C_{Y_ψ} (model with vertical tail) − C_{Y_ψ} (model without vertical tail)

$C_{n_{\psi_f}}$ = C_{n_ψ} (model with vertical tail) − C_{n_ψ} (model without vertical tail)

b model wing span

l_f model tail length arbitrarily chosen to be measured from model center of gravity to aerodynamic center of vertical tail (fig. 1) along X axis

In these computations the dynamic pressure at the tail was assumed to be equal to free-stream dynamic pressure. The values of A_e obtained by the foregoing method are given in figure 4. The increase in effective aspect ratio of the vertical tail caused by adding the horizontal tail is shown in figure 5 as a ratio of effective aspect ratio with and without the horizontal tail. The theoretical value of the ratio, computed by methods presented in reference 5, is also shown in figure 5 for comparison.

Inasmuch as the results given in figure 5 are presented as ratios, they are believed to be valid for any reasonable methods for obtaining tail area, slope of the tail lift curve, tail length, and dynamic pressure at the tail.

The increments of partial derivatives with respect to the angle of yaw of rolling-moment, yawing-moment, and lateral-force coefficients Δ_1 due to wing-fuselage interference and Δ_2 due to wing-fuselage interference on the vertical tail are shown in figures 6 to 11.

The increment Δ_1 is the difference between the slope (C_{l_ψ}, C_{n_ψ}, and C_{Y_ψ}) for the wing-fuselage combination with the horizontal tail and the sum of the slopes for the wing and for the fuselage with horizontal tail, each tested separately. Thus Δ_1 is the change in C_{l_ψ}, C_{n_ψ}, and C_{Y_ψ} caused by wing-fuselage interference for the model without the vertical tail.

The increment Δ_2 is the difference between the slope produced by the vertical tail with the wing and the

slope produced by the vertical tail without the wing. The increment Δ_2 is, therefore, the change in effectiveness of the vertical tail caused by the addition of the wing to the fuselage. The slope for the complete model may be obtained by a summation of the slopes for the component parts and the increments caused by interference. If, for example, the value of C_{n_ψ} for the complete model is desired, the following equation may be used:

$$C_{n_\psi} = C_{n_\psi}\,(\text{wing}) + C_{n_\psi}\,(\text{fuselage and both tail surfaces}) + \Delta_1 C_{n_\psi} + \Delta_2 C_{n_\psi}$$

Values of C_{l_ψ} and C_{Y_ψ} for the complete model may be obtained in a similar manner.

The values of C_{l_ψ}, C_{n_ψ}, and C_{Y_ψ} used to compute Δ_1 and Δ_2 were obtained from tests at -5° and 5° yaw by assuming a straight-line variation between those points. This assumption has been shown in reference 9 to be valid except sometimes at high angles of attack. Tailed symbols on the curves of figures 6 to 11 indicate values of slopes measured from curves of figures 12 to 15. The arrows in figures 6 and 10 indicate the direction of divergence after the stall.

The lateral-stability characteristics of the component parts of the model at high angles of yaw are given in figure 12, and the characteristics of the three wing-fuselage combinations with various tail arrangements at high angles of yaw are shown in figures 13 to 15.

DISCUSSION

General Comments

The lift, the drag, and the pitching-moment coefficients of the several model combinations are shown in figure 2. As is to be expected, the high-wing combinations have more static stability in pitch than the low-wing combinations. Inasmuch as the tests were made without wing fillets, the data for the low-wing combinations show

the effect of the burble at the wing–fuselage juncture (reference 2). The pitching-moment–coefficient curve for the midwing combination when $\delta_f = 0^\circ$ has a hump between -2° and 6° angle of attack. Comparison with figure 6 of reference 1 shows that the hump probably is a wing–fuselage effect and not the effect of the wing wake on the horizontal tail.

Lateral Stability at Small Angles of Yaw

Component parts.– The wing–alone data given in figure 3 were taken from figure 3 of reference 3, which gives also a brief discussion of the wing aerodynamic characteristics.

The addition of the horizontal tail to fuselage alone has very little effect on lateral–stability characteristics, but the addition of this surface to the fuselage with vertical tail has a pronounced effect (fig. 3). The effectiveness of the vertical tail is increased by the end–plate effect of the horizontal tail. This increased effectiveness is shown in the C_{l_ψ}, C_{n_ψ}, and C_{Y_ψ} curves (fig. 3). The increase in effective aspect ratio of the vertical tail resulting from the presence of the horizontal tail, computed from equation (1), is shown in figure 4. Figure 5 shows the ratio of effective aspect ratios with and without horizontal tail for comparison with theoretical value taken from reference 5. A considerable variation of end–plate effect with angle of attack is shown. Inasmuch as the results include the interference between the fuselage and the vertical tail as well as the end–plate effect, it is not certain whether it is the end–plate effect or the fuselage–tail interference that varies with angle of attack. Although the presence of the fuselage represents the practical case, few airplanes have a cross–sectional area as large at the tail as that represented by this model; hence, for these results an exaggeration of fuselage–tail interference is to be expected, whatever effect the interference may have. In application to design the angle of attack as given in figures 4 and 5 should be considered tail angle of attack rather than angle of attack of the airplane.

New data were taken for all fuselage–tail results because poor correlations resulted when an attempt was

made to compare the fuselage-tail data of references 1, 2, and 3 with the additional data taken for this report. Not only were comparable fuselage data taken under the same conditions, but also an improved procedure for tests and an improved method of measuring the yaw angle were used. This fact accounts for the differences existing between some of the fuselage data in the present report and data in previous reports of this series.

Wing-fuselage interference with horizontal tail in place.- The values of $\Delta_1 C_{l_\psi}$, $\Delta_1 C_{n_\psi}$, and $\Delta_1 C_{Y_\psi}$ were changed only small amounts by the addition of the horizontal tail to the wing-fuselage combinations, as shown by a comparison of figures 6, 7, and 8 with figures 4, 5, and 6 of reference 3. In general, however, the interference was decreased.

The wing-fuselage interference with horizontal tail in place contributes about 2° effective dihedral for the high wing, 3/4° for the midwing, and $-1\frac{1}{2}$° for the low wing (in fig. 6, a C_{l_ψ} of 0.0002 being considered equivalent to an effective dihedral of 1°, reference 9), with flaps retracted. With flaps deflected 60° the effective dihedral is increased 1/2° to 2°.

The values of $\Delta_1 C_{n_\psi}$ are, in general, negative; therefore the horizontal tail increased the weathercock stability (fig. 7). With flaps deflected 60° the values of $\Delta_1 C_{n_\psi}$ are also negative and, for the low wing, the tendency toward weathercock stability is considerably increased.

The values of $\Delta_1 C_{Y_\psi}$ with flaps retracted are positive for the wing in the high and low positions but negative for the wing in the midposition (fig. 8). The wing acts as a modified end plate when in the high or low positions and thus increases the side force produced by the fuselage. When flaps are deflected 60°, the value of $\Delta_1 C_{Y_\psi}$ is nearly zero except for the low-wing combination, for which it is more positive than when flaps are retracted.

Effect of wing-fuselage interference on vertical tail with horizontal tail in place.- The increment $\Delta_2 C_{l_\psi}$ is

rather small and erratic (fig. 9). The values stay within about 1° effective dihedral for the unstalled range of angle of attack. This result is in good agreement with $\Delta_2 C_{l_\psi}$ without horizontal tail (reference 3).

The increment $\Delta_2 C_{n_\psi}$ is negative (increases weathercock stability) for the low wing, but becomes less negative (less weathercock stability) as the wing is moved up to the middle position and becomes positive (decreases weathercock stability) for some of the high-wing conditions (fig. 10). This same trend for $\Delta_2 C_{n_\psi}$ is true for the horizontal-tail-off condition, but it should be noted that the difference between numerical values due to vertical location of the wing is only about one-half as great when the horizontal tail is in place.

The reduction of the difference in the interference between high- and low-wing models is again apparent in $\Delta_2 C_{Y_\psi}$ when the horizontal tail is present (fig. 11).

The early break in the low-wing curves of $\Delta_1 C_{l_\psi}$, $\Delta_1 C_{n_\psi}$, and $\Delta_2 C_{n_\psi}$ for $\delta_f = 0°$ at about 10° angle of attack is caused by a burble developing at the wing-fuselage juncture as explained in previous reports of this series.

Lateral Stability at Large Angles of Yaw

Fuselage and tail combinations.- Although rather erratic, the C_l curves (fig. 12) are consistent in that those combinations which have weathercock stability have more effective dihedral at low angles of attack; whereas those combinations which do not have weathercock stability have more effective dihedral at high angles of attack. Although the horizontal tail improves the effectiveness of the vertical tail at small angles of yaw, a more sudden break occurs in the curves at angles of yaw greater than 10°; therefore, at large angles of yaw the vertical tail is less effective when the horizontal tail is present, as shown by the C_n and C_Y curves.

Complete model.- The addition of the horizontal tail to the complete model has only small effects on C_l compared with the effect of a change in the vertical position

of the wing or the addition of the vertical tail (fig. 13). The effect of those model changes on C_l has previously been discussed in reference 3.

The curves for C_n with the wing present (fig. 14) show again that the end-plate effect of horizontal tail on the vertical tail is detrimental to the restoring moment in yaw for angles of yaw greater than about 25°. The addition of the wings to the fuselage gave a substantial increase in the restoring moment in yaw at large angles of yaw and increased the weathercock stability at small angles of yaw (figs. 12 and 14).

A pronounced break in the C_n and C_Y curves of the fuselage with the horizontal tail that occurred at a high angle of attack (fig. 12) between 25° and 30° yaw vanishes when the wing is added. The break may have been caused by the unstalling of the horizontal tail as its resultant angle of attack is reduced by yaw — that is, the angle of attack measured in a plane parallel to the plane of symmetry of the unyawed model. When the wing is present, the downwash probably prevents the tail from stalling for any portion of the yaw range.

Curves for C_Y (fig. 15) show larger values at large angles of yaw when the horizontal tail is absent; this fact is in agreement with what has been shown by curves for C_n with the wing and curves for C_n and C_Y without the wing.

CONCLUSIONS

The results of tests of a model consisting of a circular fuselage, tail surfaces, and a wing in high, middle, and low positions indicate that:

1. The effective aspect ratio of the vertical tail as determined from lateral force on the vertical tail was increased from 20 to 60 percent by the addition of the horizontal tail, depending on the angle of attack.

2. For angles of yaw greater than about 15°, the presence of the horizontal tail decreased the restoring moment in yaw contributed by the vertical tail.

3. The vertical-tail effectiveness increased as the wing was moved from the high to the low position; the low-wing combination therefore had the most weathercock stabil-

ity. The addition of the horizontal tail reduced the change in vertical-tail effectiveness with wing position about 50 percent, with the result that the high- and low-wing models possessed more nearly the same weathercock stability.

Langley Memorial Aeronautical Laboratory,
National Advisory Committee for Aeronautics,
Langley Field, Va.

REFERENCES

1. House, Rufus O., and Wallace, Arthur R.: Wind-Tunnel Investigation of Effect of Interference on Lateral-Stability Characteristics of Four NACA 23012 Wings, an Elliptical and a Circular Fuselage, and Vertical Fins. Rep. No. 705, NACA, 1941.

2. Recant, Isidore G., and Wallace, Arthur R.: Wind-Tunnel Investigation of Effect of Yaw on Lateral-Stability Characteristics. III - Symmetrically Tapered Wing at Various Positions on Circular Fuselage with and without a Vertical Tail. T.N. No. 825, NACA, 1941.

3. Recant, I. G., and Wallace, Arthur R.: Wind-Tunnel Investigation of Effect of Yaw on Lateral-Stability Characteristics. IV - Symmetrically Tapered Wing with a Circular Fuselage Having a Wedge-Shaped Rear and a Vertical Tail. NACA A.R.R., March 1942.

4. Recant, Isidore G., and Wallace, Arthur R.: Wind-Tunnel Investigation of the Effect of Vertical Position of the Wing on the Side Flow in the Region of the Vertical Tail. T.N. No. 804, NACA, 1941.

5. Katzoff, S., and Hutterperl, William: The End-Plate Effect of a Horizontal-Tail Surface on a Vertical-Tail Surface. T. N. No. 797, NACA, 1941.

6. Harris, Thomas A.: The 7 by 10 Foot Wind Tunnel of the National Advisory Committee for Aeronautics. Rep. No. 412, NACA, 1931.

7. Wenzinger, Carl J., and Harris, Thomas A.: Wind-Tunnel Investigation of an N.A.C.A. 23012 Airfoil with Various Arrangements of Slotted Flaps. Rep. No. 664, NACA, 1939.

8. Jones, Robert T.: Correction of the Lifting-Line Theory for the Effect of the Chord. T.N. No. 817, NACA, 1941.

9. Bamber, M. J., and House, R. O.: Wind-Tunnel Investigation of Effect of Yaw on Lateral-Stability Characteristics. I - Four N.A.C.A. 23012 Wings of Various Plan Forms with and without Dihedral. T.N. No. 703, NACA, 1939.

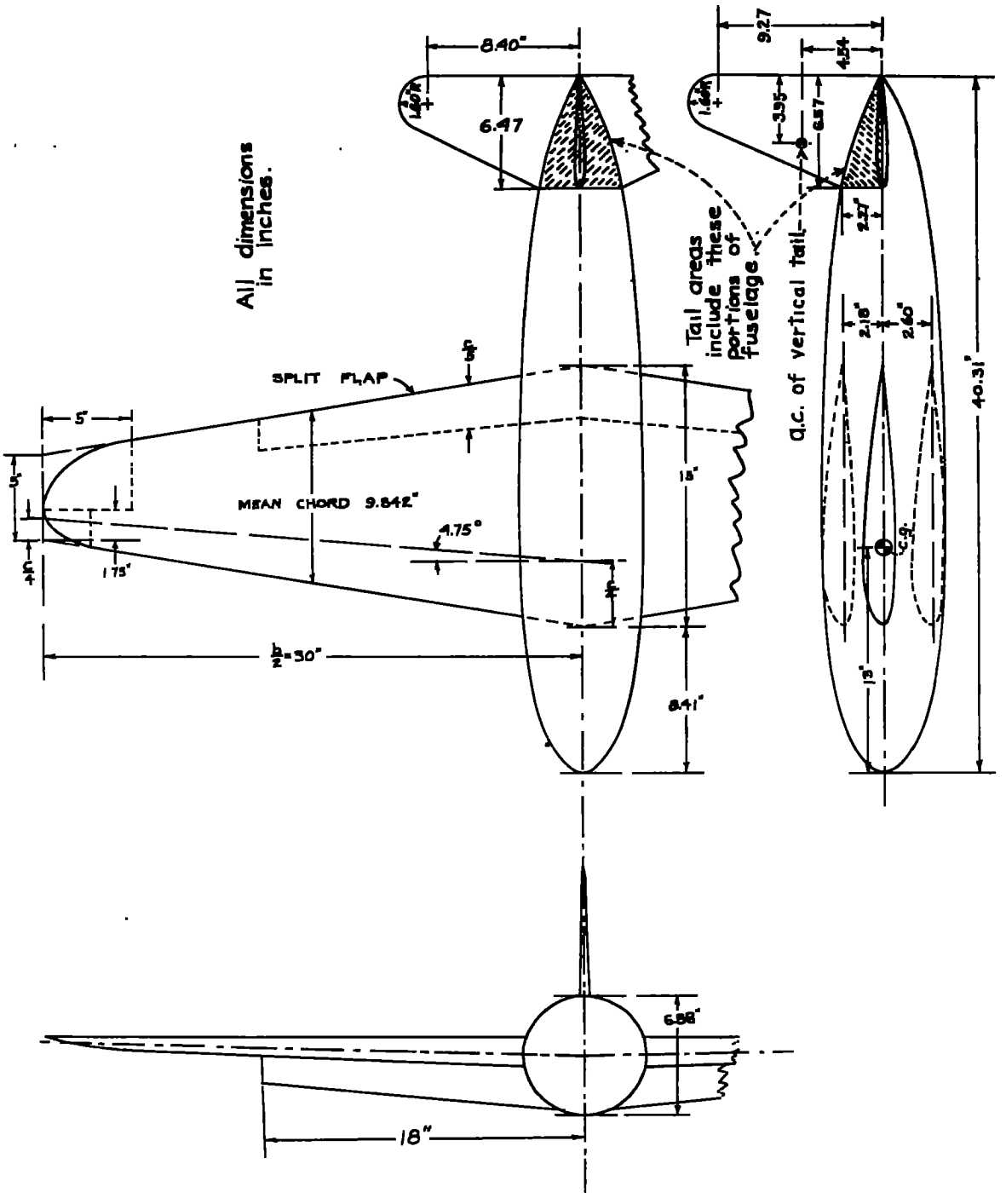

Figure 1.—Drawing of NACA 23012 wing in combination with circular fuselage and horizontal and vertical tail of NACA 0009 section.

NACA

Fig. 2a

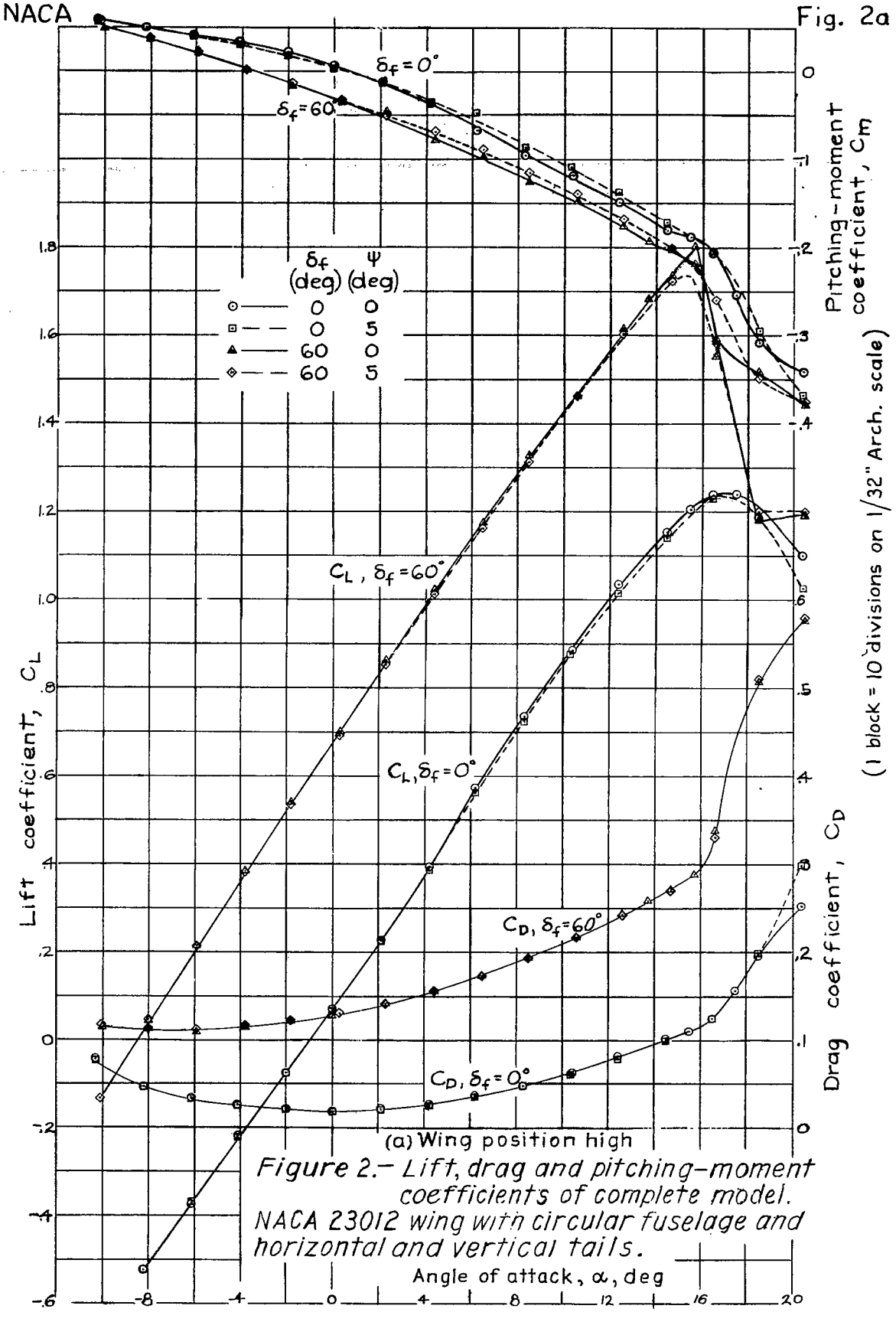

Figure 2.– Lift, drag and pitching-moment coefficients of complete model. NACA 23012 wing with circular fuselage and horizontal and vertical tails.

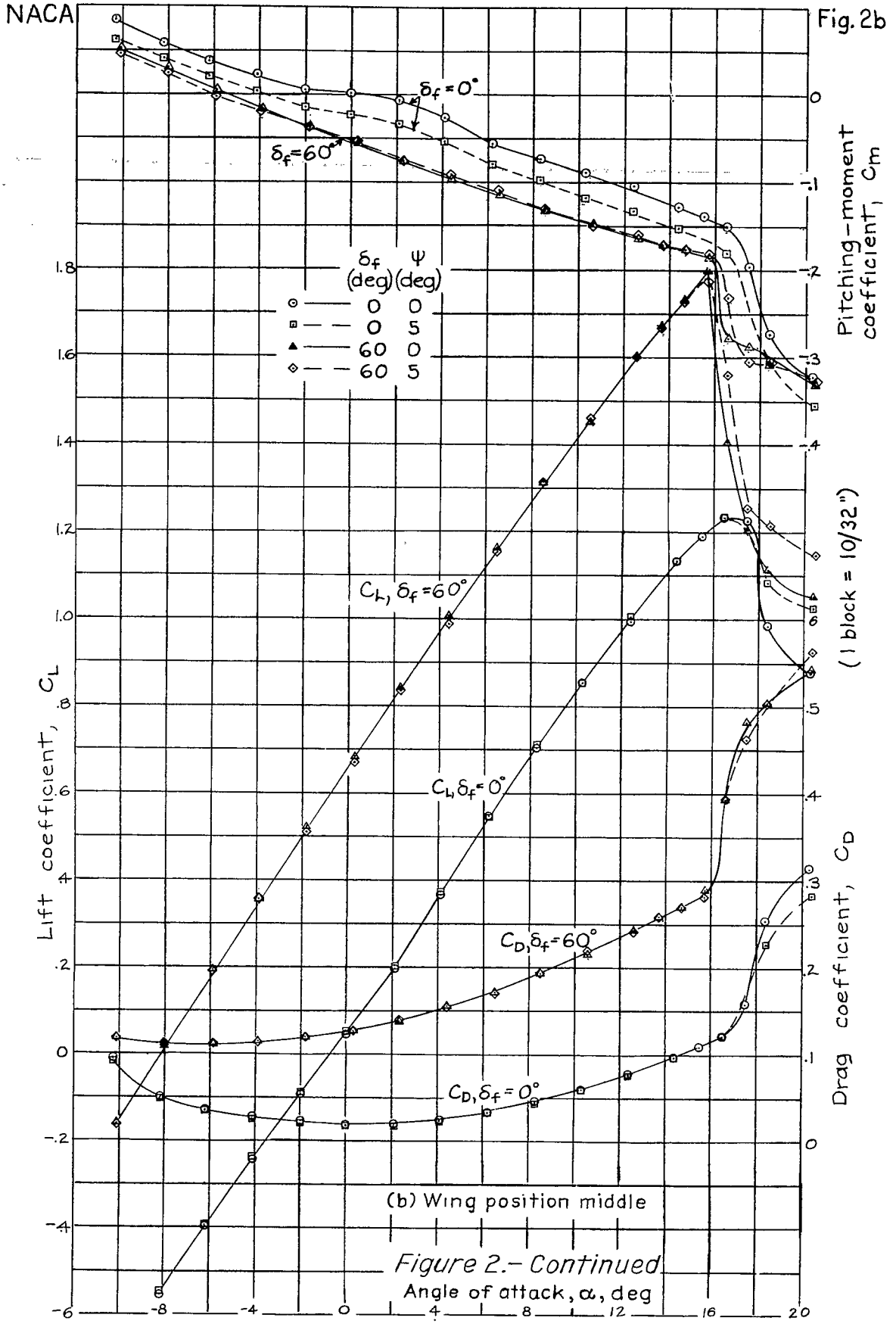

Figure 2.- Continued

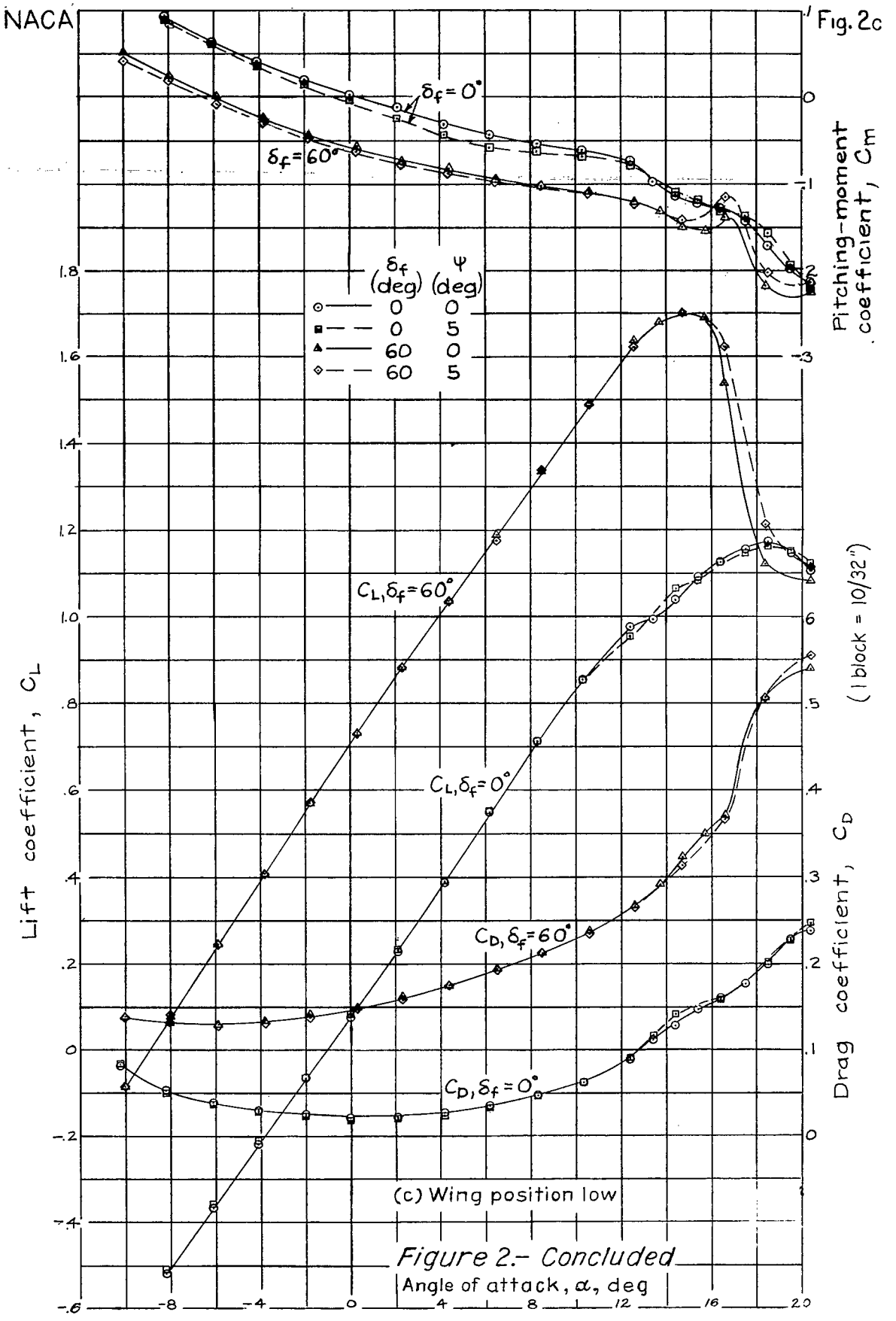

Figure 2.- Concluded

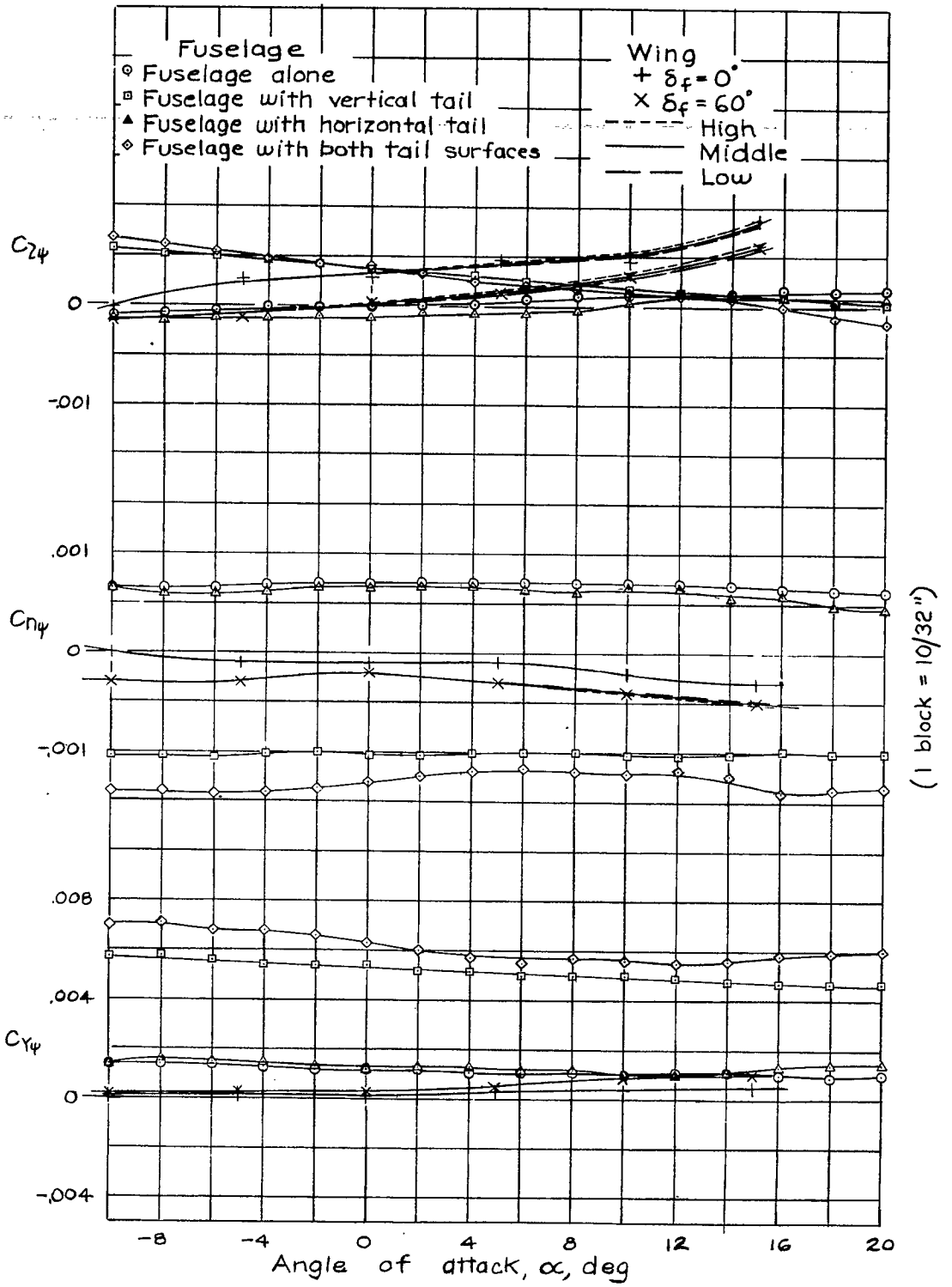

Figure 3.—Variation of C_{ℓ_ψ}, C_{n_ψ}, and C_{y_ψ} with angle of attack.

NACA 23012 wing alone, fuselage, and fuselage with tail surfaces. (Data for wing from reference 3.)

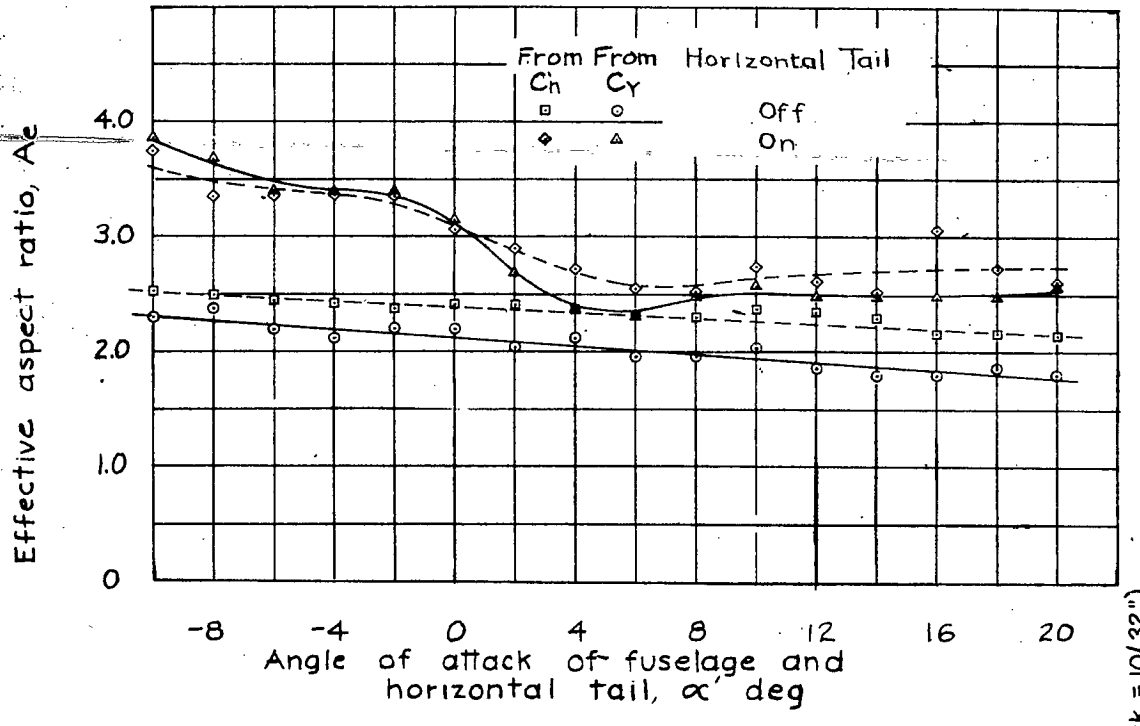

Figure 4.- Effective aspect ratio of vertical tail on circular fuselage. (Geometric aspect ratio, 2.2.)

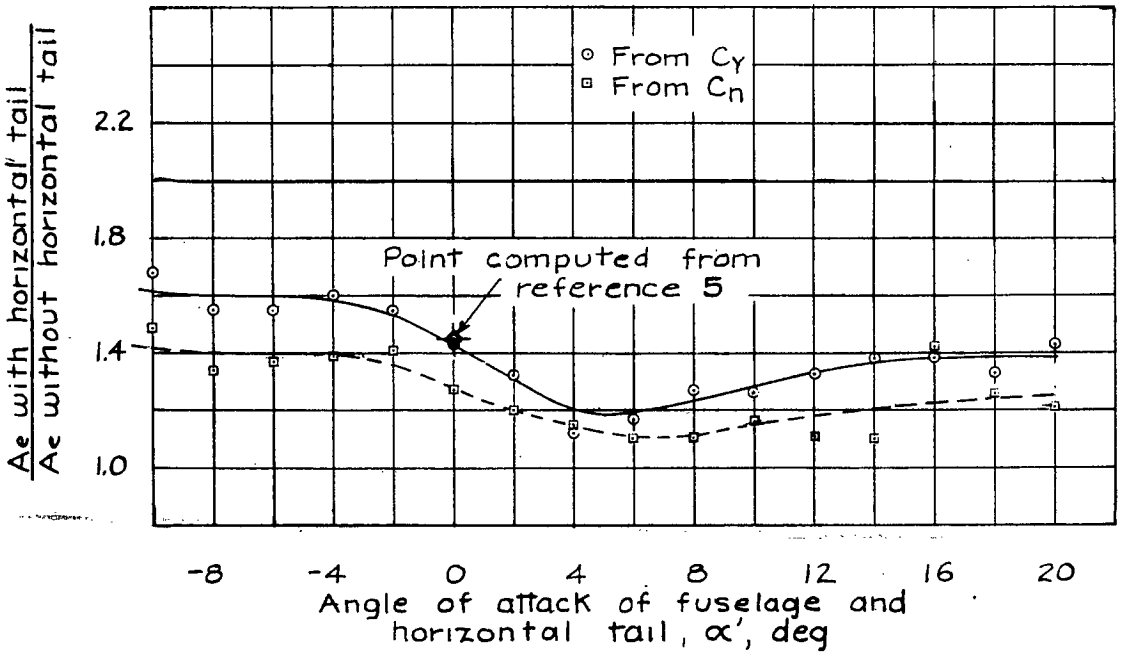

Figure 5.- Ratio of effective aspect ratio of vertical tail on the circular fuselage with horizontal tail to that without horizontal tail.

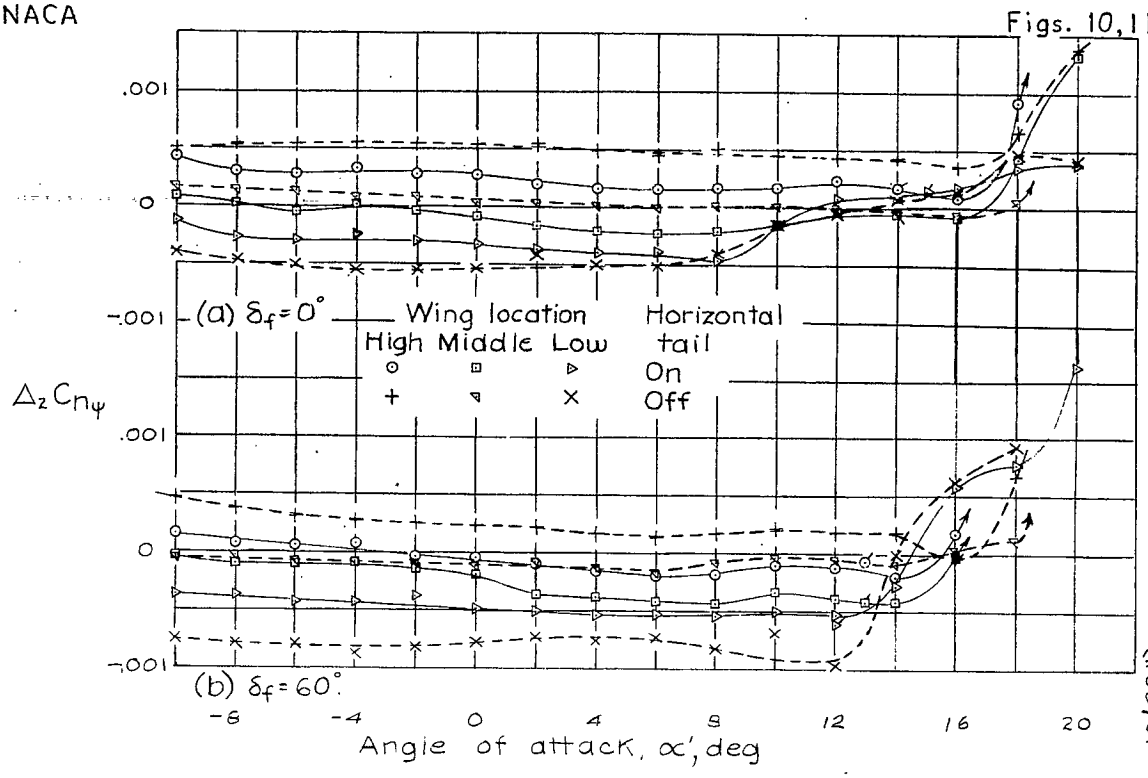

Figure 10.- Effect of wing-fuselage interference on C_{n_ψ} due to vertical tail. NACA 23012 wing with fuselage and horizontal and vertical tails. (Data with horizontal tail off from reference 3.)

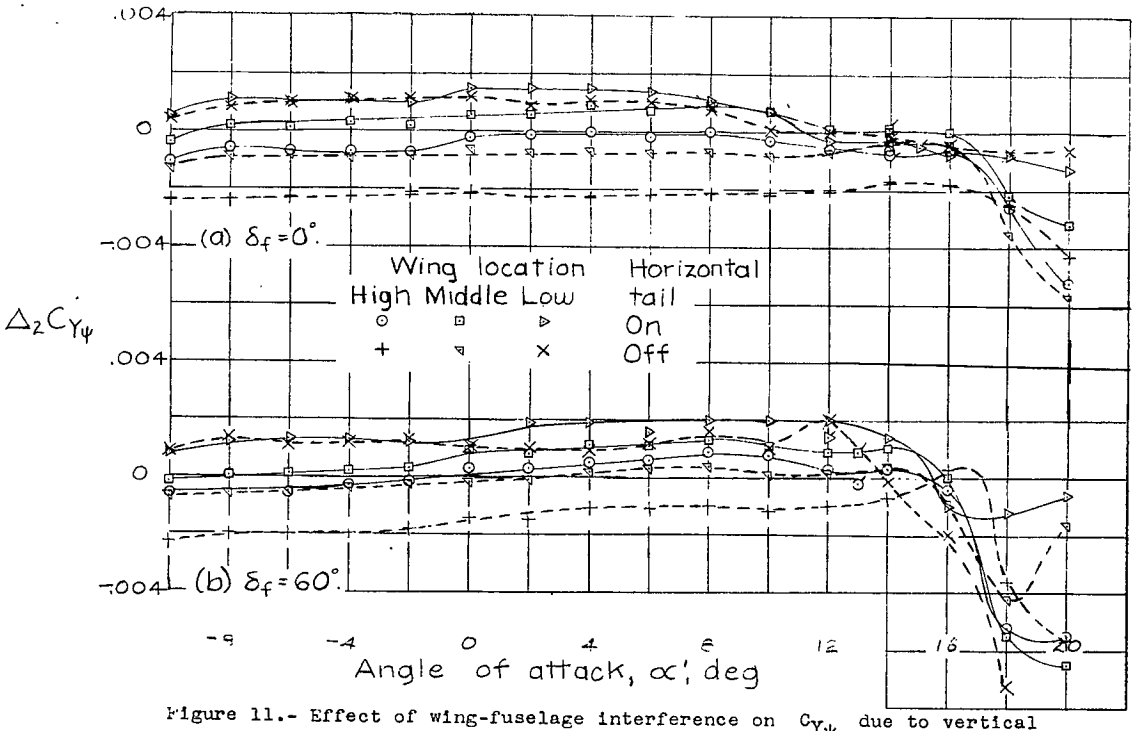

Figure 11.- Effect of wing-fuselage interference on C_{Y_ψ} due to vertical tail. NACA 23012 wing with fuselage and horizontal and vertical tails. (Data with horizontal tail off from reference 3.)

NACA

Fig. 12

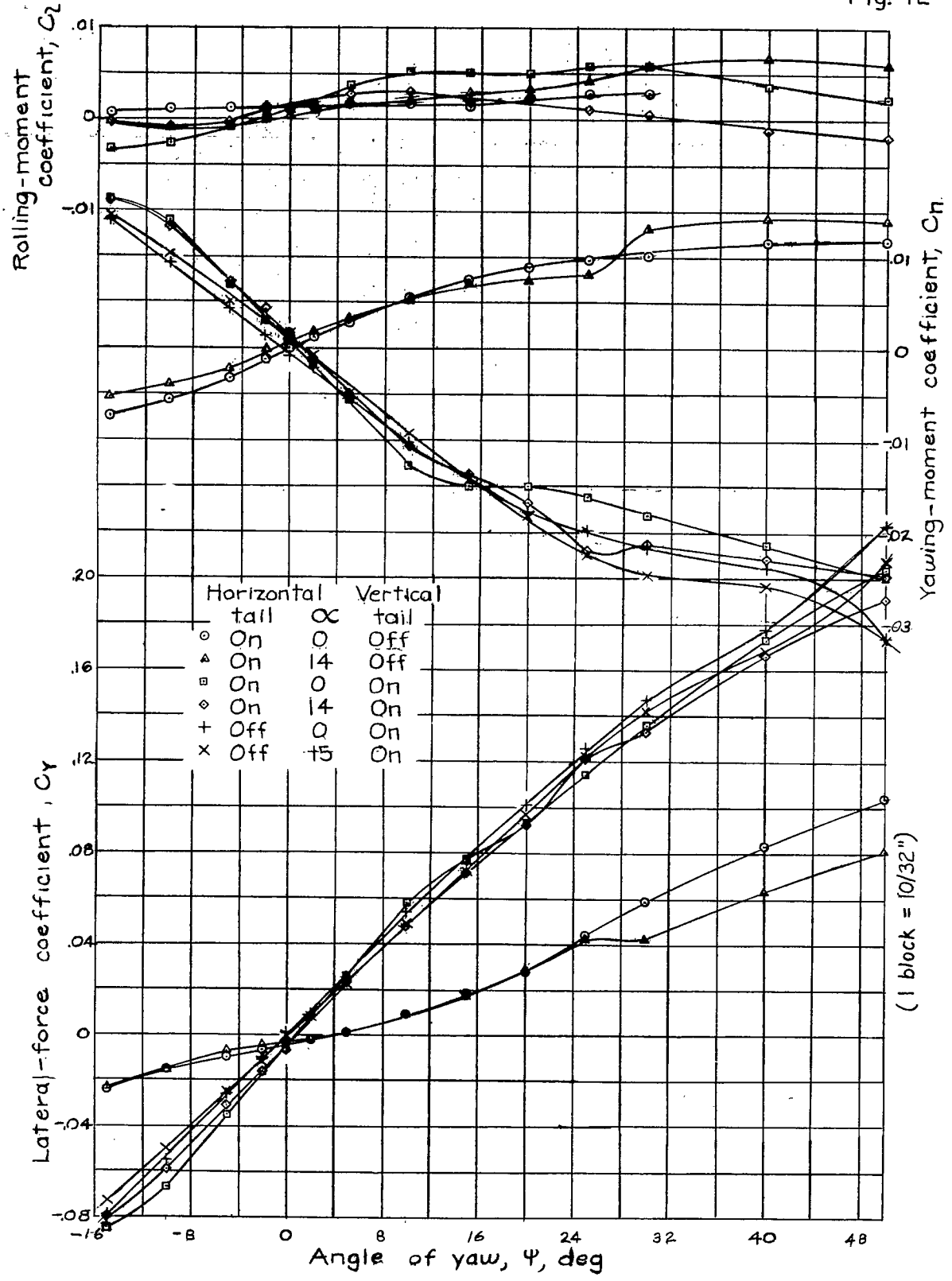

Figure 12.—Variation of C_l, C_n, and C_Y with angle of yaw. Fuselage and fuselage with tail surfaces.

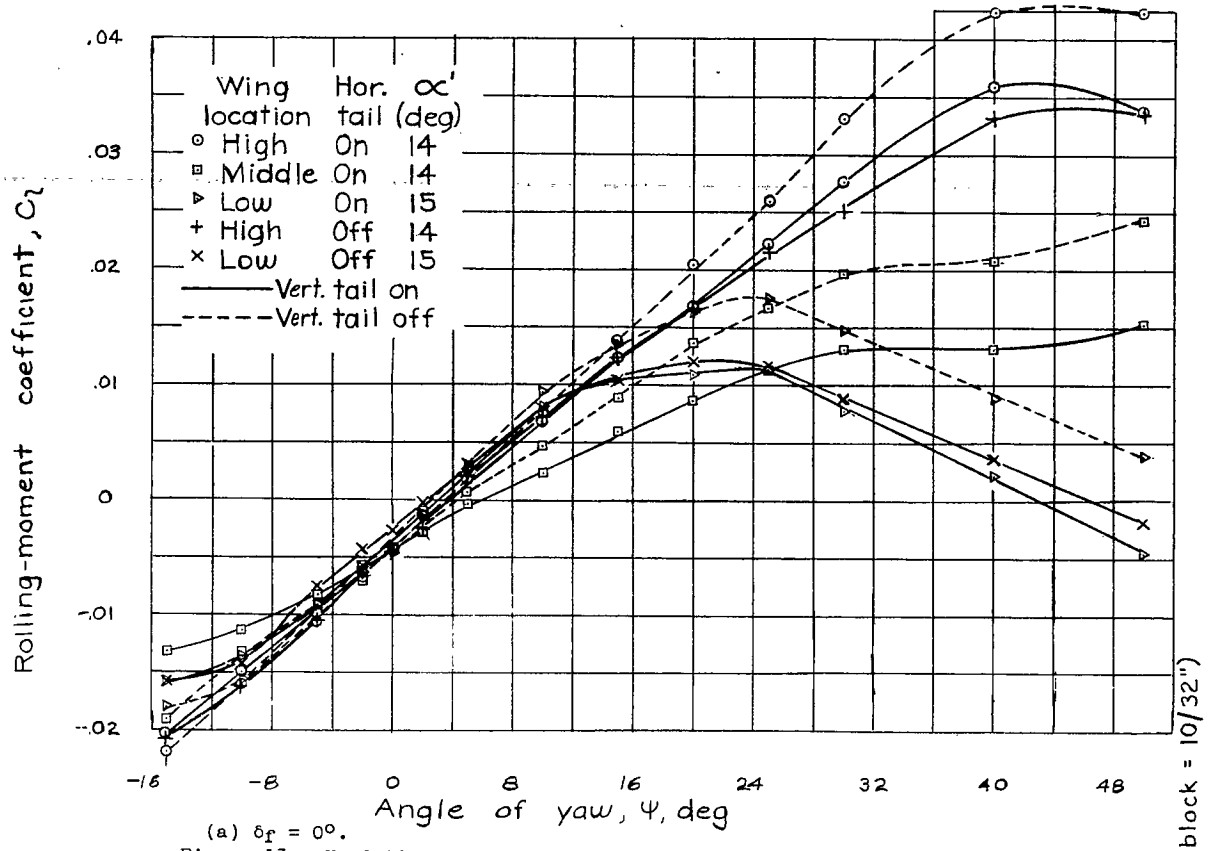

(a) $\delta_f = 0°$.

Figure 13.- Variation of rolling-moment coefficient with yaw. NACA 23012 wing with fuselage and horizontal and vertical tails.

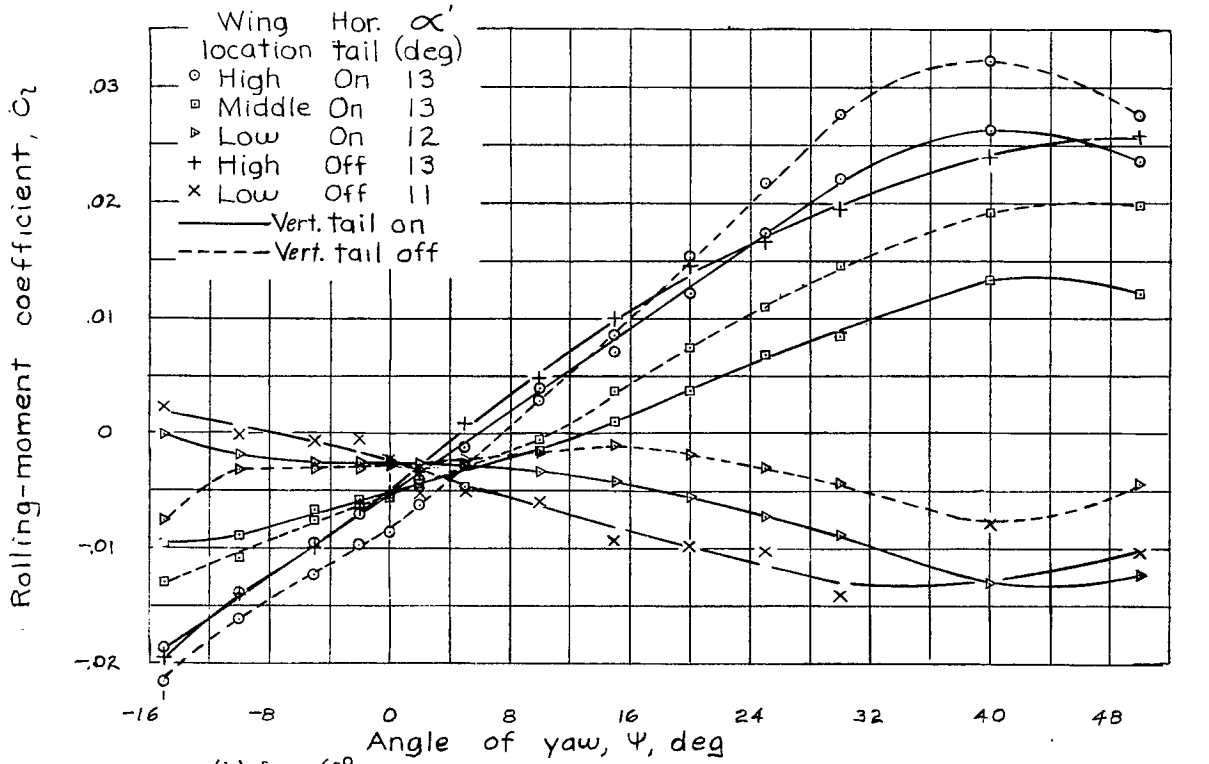

(b) $\delta_f = 60°$.

Figure 13.- Concluded.

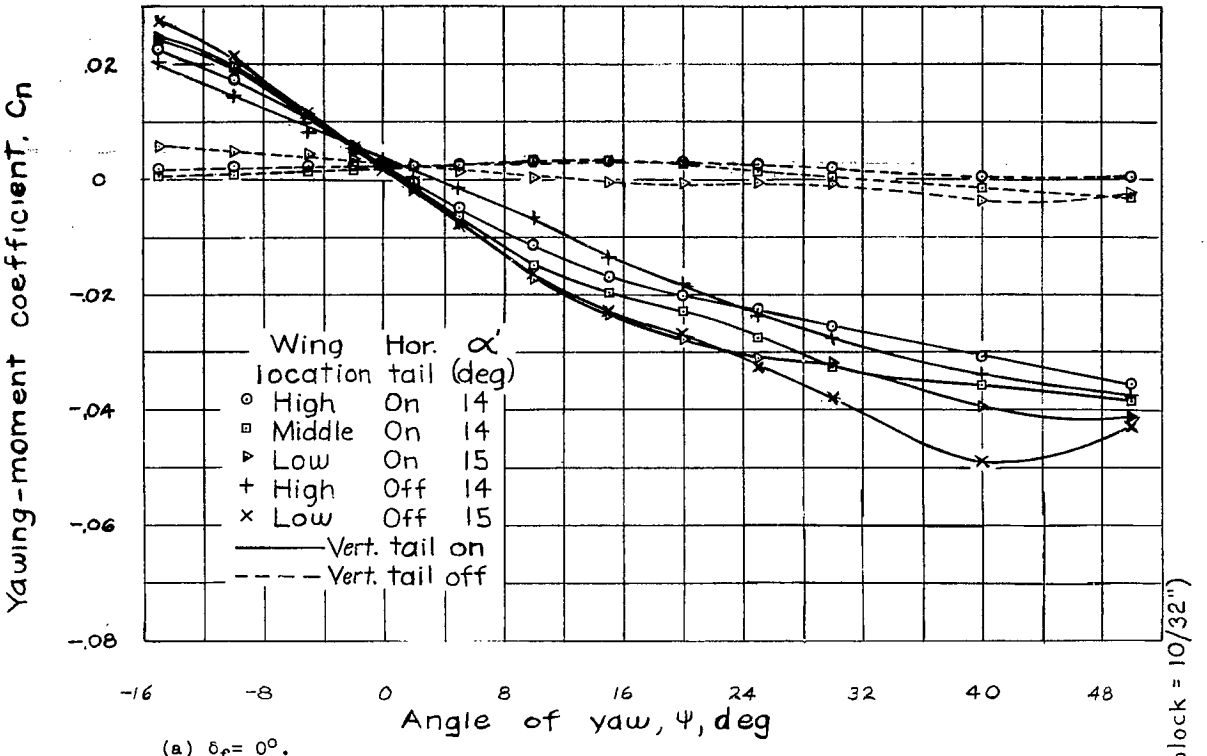

(a) $\delta_f = 0°$.

Figure 14.- Variation of yawing-moment coefficient with yaw. NACA 23012 wing with fuselage and horizontal and vertical tails.

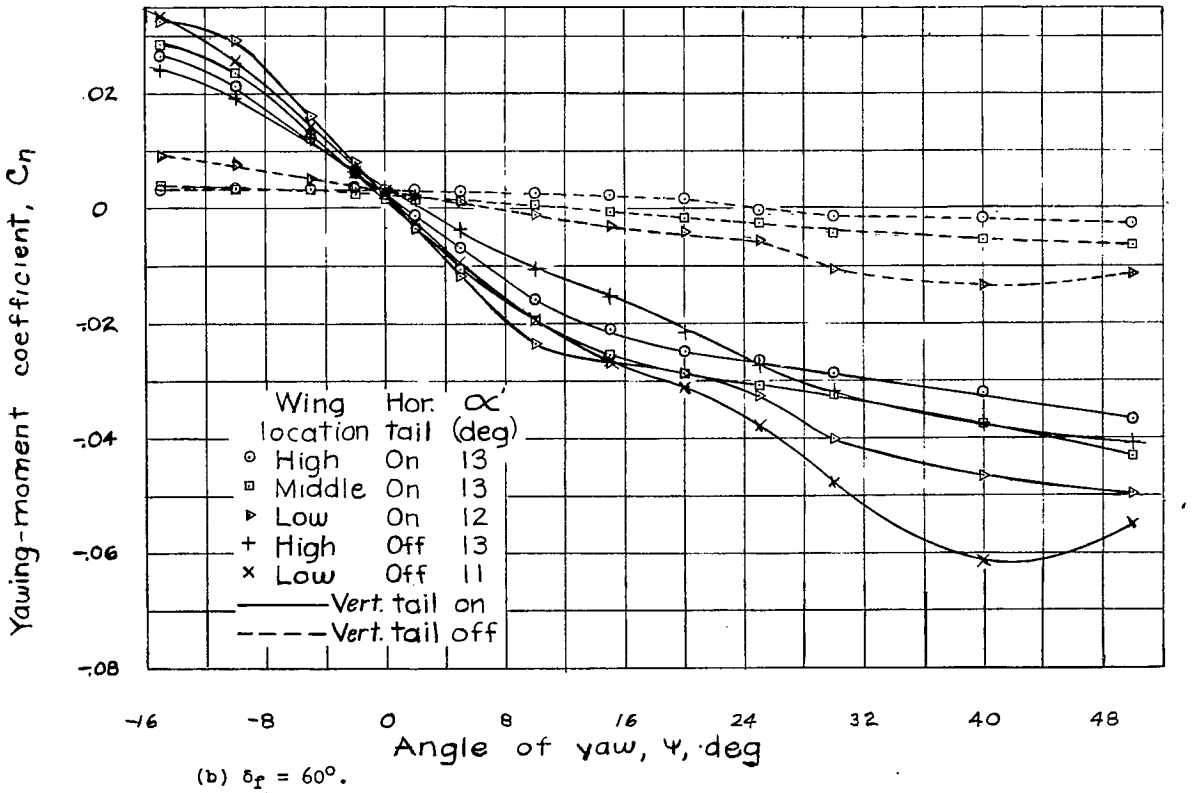

(b) $\delta_f = 60°$.

Figure 14.- Concluded.

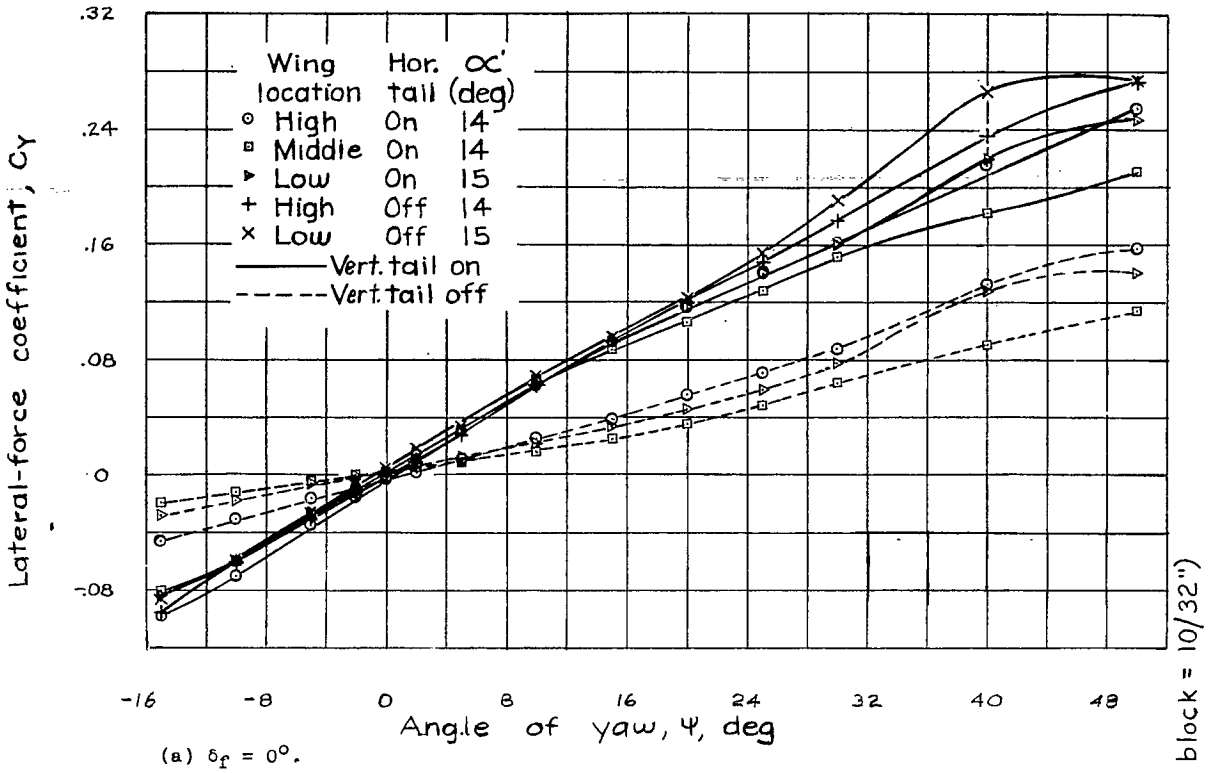

(a) $\delta_f = 0°$.

Figure 15.- Variation of lateral-force coefficient with yaw. NACA 23012 wing with fuselage and horizontal and vertical tails.

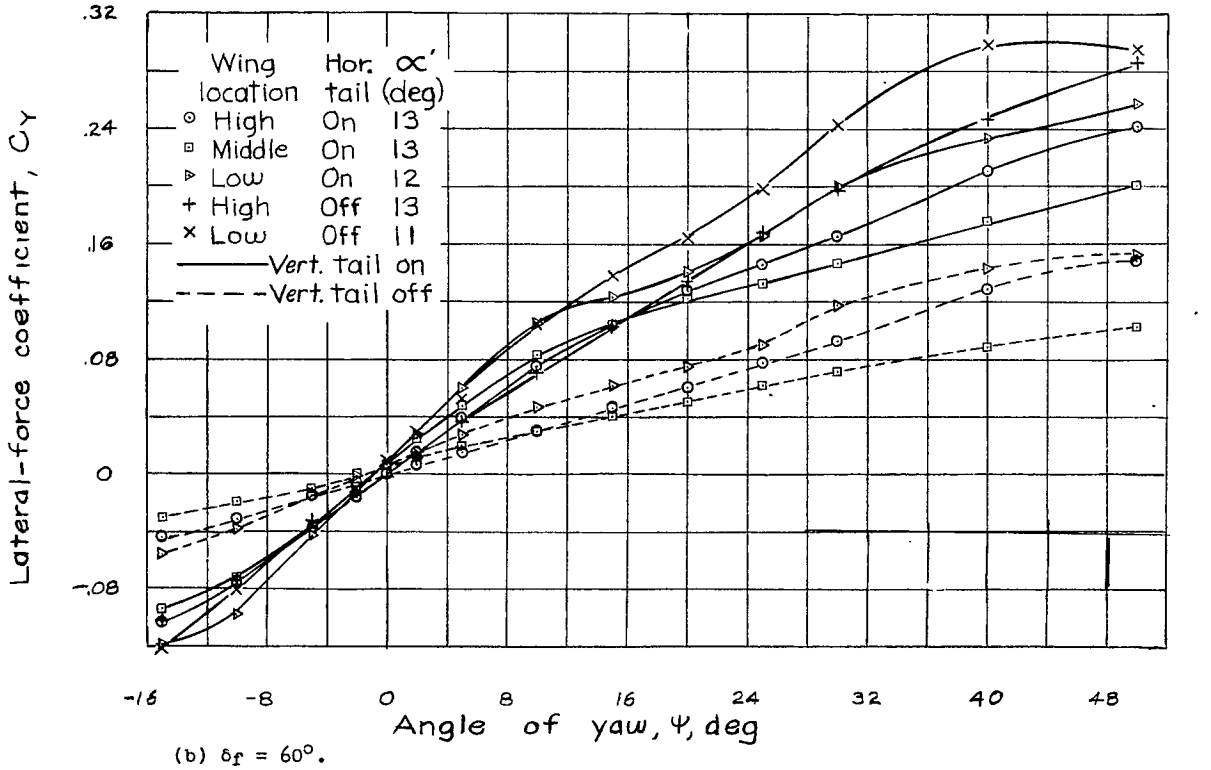

(b) $\delta_f = 60°$.

Figure 15.- Concluded.